

1
2
3
4
5
6
7
8
9
10
11
12
13
14
15
16
17
18
19
20
21
22
23
24
25
26
27
28
29
30
31
32
33
34

Revision 2

Adsorption of sulfur dioxide on volcanic ashes

DEBORAH SCHMAUSS AND HANS KEPPLER*

Bayerisches Geoinstitut, Universität Bayreuth, 95440 Bayreuth, Germany

* E-mail: Hans.Keppler@uni-bayreuth.de

ABSTRACT

The adsorption of pure sulfur dioxide gas on volcanic ashes has been studied from 0.1 mbar to 1 bar and from - 80 °C to + 150 °C. Finely ground synthetic glasses of andesitic, dacitic and rhyolitic composition served as proxies for fresh natural ash surfaces. Powders from two natural obsidian samples were also studied and yielded results broadly similar to the synthetic model systems. SO₂ adsorption on ash is partially irreversible; it appears that the first layer of SO₂ molecules absorbed on the surface cannot be removed. The pressure and temperature dependence of adsorption can be described by the equation $\ln c = A T^{-1} + B \ln p + C$, where c is the surface concentration of adsorbed SO₂ in mg/m², T is temperature in Kelvin and p is the partial pressure of SO₂ in mbar. A multiple regression analysis of the experimental data yielded $A = 1645$, $B = 0.29$, $C = - 7.43$ for andesite, $A = 2140$, $B = 0.29$, $C = - 9.32$ for dacite and $A = 910$, $B = 0.21$, $C = - 4.48$ for rhyolite. These data imply that adsorption strongly decreases with temperature, but only slowly decreases with decreasing partial pressure of SO₂. Therefore, adsorption primarily occurs in the cool and diluted parts of the volcanic plume. Model calculations show that most of the SO₂ may be removed from the plume, if the initial SO₂ concentration in the volcanic gases is low and the surface area of the ash is high. For high initial SO₂ concentrations, the fraction of SO₂ that is lost by adsorption decreases, since the amount of SO₂ in the gas phase is proportional to the SO₂ partial pressure p , while adsorption is proportional only to $p^{0.2} - p^{0.3}$. Adsorption of SO₂ on ash particles may therefore be one reason why the climatic impact of explosive volcanic eruptions does not always scale with total sulfur yield.

Keywords: sulfur dioxide, volcanic gases, ashes, adsorption

INTRODUCTION

35
36 Volcanoes interact with the atmosphere in a variety of ways (McCormick et al. 1995;
37 Mather 2008; Robock, 2000). During some explosive eruptions, sulfur dioxide is
38 injected into the stratosphere, where it is photochemically oxidized to sulfate aerosols,
39 which absorb sunlight and cool global surface temperatures (Bluth et al. 1993;
40 McCormick et al. 1995; Briffa et al. 1998; de Silva and Zielinski 1998; Robock 2000;
41 Robock et al. 2009). Local ozone depletion may be related to halogens or to ash
42 particles in the eruption plumes (McCormick et al. 1995; Textor et al. 2003; Rose et
43 al. 2006). While ash particles probably have only a short-term effect on climate, their
44 environmental impact is considerable. They may fertilize seawater (Frogner et al.
45 2001; Jones and Gislason 2008) or, depending on their composition, have toxic effects
46 on vegetation, animals, and humans (Oskarsson 1980). In addition, ashes pose a
47 severe hazard for aviation (e.g. Guffanti et al. 2010). Chemical interaction between
48 ashes and gases in the eruption cloud is essential for understanding all of these
49 phenomena. The surface of ashes is often highly enriched in sulfur and halogens,
50 which is believed to be due to adsorption of HCl, HF and SO₂ (Rose 1977; Oskarsson
51 1980; Witham et al. 2005; Delmelle et al. 2007; Bagnato et al. 2013). Adsorption
52 processes are important for the following reasons: (1) Adsorption of SO₂ and halogens
53 on ashes will reduce the amount of climate-relevant gases delivered to the
54 stratosphere, since ashes usually sediment within a few days back to the surface. (2)
55 Adsorbed gas species and their reaction products are the main cause for the toxicity of
56 ashes (e.g. Oskarsson 1980) and they may also contribute to the corrosion of aircraft
57 engines. (3) Leachates of ashes are often used as a proxy for volcanic gas chemistry
58 (Witham et al. 2005; Bagnato et al. 2011). However, a recent study by Bagnato et al.
59 (2013) showed that the ratios of S, F, and Cl adsorbed on ashes of the 2010
60 Eyafjallajökull eruption are very different from the corresponding gas ratios measured
61 in the plume. Therefore, the ratios of halogens and sulfur as determined from
62 leachates can only be translated into gas compositions, if the adsorption isotherms,
63 which relate the amount of absorbed gas to its partial pressure, are known. (4) Ash
64 particles provide reactive surfaces in volcanic plumes that may catalyze various
65 chemical reactions between gas species (e.g. Jordan et al. 2000). Adsorption of the
66 surface of the particle is likely the first step in such a process.
67

68 Among volcanic gas species, sulfur compounds likely have the strongest
69 environmental impact, as they are responsible for the formation of sulfate aerosols
70 that may remain in the stratosphere for years. SO₂ is likely the most abundant sulfur
71 species in plumes, with H₂S occurring only at very low oxygen fugacities; however,
72 very oxidized arc magmas may release some of their sulfur directly in hexavalent
73 form (likely as H₂SO₄ or sulfate; Binder and Keppler 2011; Ni and Keppler 2012).
74 Unlike HCl, which is highly soluble in water and therefore easily removed by
75 condensed water droplets, liquid films on particles or by ice (e.g. Textor et al. 2003),
76 SO₂ is poorly soluble in water and adsorption on ashes may therefore be the main
77 mechanism for depleting it from volcanic plumes after eruption. The change in plume
78 SO₂ content has been directly observed in several recent eruptions, either by ground-
79 based or satellite spectrometers; the data indicate that losses of 50 % or more within a
80 few days are common, with loss rates varying widely (e.g. Rodriguez et al. 2008;
81 Krotkov et al. 2010). In the stratosphere, SO₂ is ultimately converted into sulfate
82 aerosols. The rate of this reaction, however, is limited by the low abundance of the
83 OH radical, which is involved in the initial and rate-limiting step of the reaction chain.
84 The characteristic time scale for the conversion of SO₂ to sulfate is in the order of tens
85 of days, and even longer for high sulfur loading (Bekki 1995). Accordingly, this
86 process cannot be responsible for any rapid loss of SO₂ from the cloud.

87
88 Experimental data on the interaction of SO₂ with the surface of ash particles are very
89 limited. Ayris et al. (2013) studied the interaction of tephra with SO₂ and suggested
90 that sulfur may be removed from the gas phase by the diffusion of Ca²⁺ to the surface
91 of the glass particles followed by the precipitation of CaSO₄. As the diffusion of Ca²⁺
92 is strongly temperature dependent, this process may only occur at high-temperature,
93 near vent conditions or inside the vent. Indeed, Ayris et al. (2013) conclude that this
94 scavenging mechanism is only significant if fragmentation of the magma occurs more
95 than 500 meters below the surface. However, the study of Bagnato et al. (2013)
96 showed a major increase of adsorbed sulfur with distance from the vent for the 2010
97 Eyjafjallajökull eruption, which suggests that most of the sulfur scavenging occurs at
98 rather low temperatures in the volcanic plume at high altitude. The interaction
99 between SO₂ and ashes under these low-temperature conditions is hardly studied (Gu
100 et al., 1999). We therefore present here a systematic experimental study of SO₂
101 adsorption on volcanic ashes, from - 80 °C to + 150 °C, and from 0.1 mbar to 1 bar

102 SO₂ pressure. Our study therefore covers most of the temperature and SO₂ partial
103 pressure range that is expected for the cool, dilute parts of a volcanic plume (e.g.
104 Textor et al. 2003, 2006). As a proxy of fresh, unweathered volcanic ash we used fine
105 powders of both synthetic and natural silicate glasses. While ash is a mixture of
106 various materials, including fine rock fragments, crystals and glasses, it is likely that
107 fresh amorphous glass surfaces with their high defect population are the preferred
108 sites of adsorption (e.g. Rendulic 1988; Leed and Pantano 2003). In particular for
109 explosive, intermediate to silicic eruptions, glassy material is usually the dominant
110 constituent of fresh ash.

111

112

113 **EXPERIMENTAL METHODS**

114

115 **Sample preparation**

116 Fe-free andesite, dacite and rhyolite glasses were prepared from mixtures of high-
117 purity (> 99.9 wt. %) SiO₂, Al(OH)₃, Mg(OH)₂, CaCO₃, Na₂CO₃, and K₂CO₃. They
118 were mixed in a planetary mill under ethanol and then slowly heated in a platinum
119 crucible to 1100 °C for decarbonation and dehydration. The charges were then melted
120 at 1600 °C in a high temperature furnace for 2 hours and quenched in water. The
121 glasses produced contained some bubbles, but were free of crystals. Chemical
122 compositions are given in Table 1. The glasses were then ground in a planetary mill
123 for 5 – 10 min without adding any liquid, to avoid adsorption on the fresh surfaces.
124 The surface area of the powders was determined using a Micrometrics Gemini III
125 2375 surface analyzer by measuring the BET adsorption isotherm of nitrogen
126 (Brunauer et al. 1938). Surface areas obtained were in the range of 2600 – 4500
127 m²/kg, which implies an average grain size in the order of 0.6 – 1 μm. This is
128 comparable to the low grain-size fraction of natural ashes (e.g. Carey and Sigurdsson
129 1982). For some experiments, natural obsidian glasses from Lipari (Aeolian Islands,
130 Italy; rhyolitic composition) and from Puu Waawaa (Hawaii; trachytic composition)
131 were ground up to fine powders in the same way as the synthetic samples. The
132 synthetic samples were chosen to be iron-free to avoid complications arising from
133 possible redox reactions between ferric iron and SO₂; the natural glasses were studied

134 to test whether the adsorption isotherms measured for the synthetic samples are
135 comparable to those of natural compositions.

136

137 **Adsorption and desorption experiments**

138 Adsorption and desorption measurements were carried out in a glass apparatus shown
139 in Fig. 1. Pressure in the apparatus was measured by a Vacuubrand DVR 5 vacuum
140 gauge with an Al₂O₃-coated pressure transducer that is inert to SO₂. The pressure
141 transducer is a plate capacitor, which transforms mechanical deformation due to
142 external pressure into a change of capacity. The instrument has a measurement range
143 of 0.1 mbar to 1 bar, with an accuracy of ± 0.1 mbar up to 10 mbar and ± 1 mbar up to
144 1 bar.

145

146 At the beginning of an experiment 30 – 50 g of finely ground glass powder was
147 placed in the sample tube and the entire system was evacuated to < 0.1 mbar for
148 several hours with a rotary vane pump (Vacuubrand RZ6). A liquid nitrogen-cooled
149 cold trap was placed between the pump and the apparatus in order to avoid
150 contamination of the sample by oil fumes and to protect the pump from any gases
151 released from the samples. After switching off the vacuum pump, the pressure in the
152 system was observed for several hours to check for leaks. Only if pressure remained
153 at < 0.1 mbar, the experiment was continued. After this, the valve to the sample was
154 closed and the round flask was filled with a desired pressure of SO₂ from the gas
155 bottle. The two washing flasks filled with paraffin as shown in Fig. 1 served as a
156 safety valve to avoid any overpressure inside the glass apparatus. When the valve
157 connecting the sample with the gas reservoir was opened, first a small, instantaneous
158 pressure drop occurred because of the increase in available gas volume. This was
159 followed by a continuous decrease in pressure due to absorption of SO₂ on the ash
160 surface. Most of the decrease occurred rapidly within the first 10 – 30 minutes. After
161 a few hours, pressure kept decreasing only very slightly and after one or two days, it
162 remained constant, indicating that equilibrium between gas and ash surface had been
163 reached. We carried out some long-time experiments with durations up to two weeks;
164 they showed no further change of pressure in the system. From the value of
165 equilibrium pressure achieved after one or two days and its difference to the original
166 pressure, the amount of adsorbed SO₂ can be calculated.

167

168 A measurement cycle always started with adsorption at low pressure. After
169 equilibrium had been reached, the valve to the sample was closed and a higher
170 pressure of gas was filled into the reservoir and the absorption experiment was
171 repeated. Several adsorption experiments were carried out in steps until a final
172 pressure near 1 bar was reached. After this, the valve between sample and reservoir
173 was closed and the pressure of SO₂ in the round flask was reduced by means of the
174 rotary vane pump. After opening the valve between sample and reservoir, first a
175 slight increase in pressure occurred because of the higher gas pressure in the sample
176 tube, followed by a continuous increase in pressure due to desorption of SO₂ from the
177 ash surface. Again, after a few hours, a steady state indicating equilibrium was
178 reached. The desorption step was then repeated several times with decreasing
179 pressures, until nearly zero mbar were reached. Experiments at variable temperature
180 were carried out by immersing the sample container in an oil bath or in a cooling
181 mixture.

182
183 In order to quantify adsorption, three volumes in the system need to be known
184 precisely: V₁, the volume of the gas reservoir (round glass flask plus glass tubing
185 attached to it), V₂, the volume of the empty sample tube and V₃, the empty gas space
186 in the sample tube after filling it with glass powder. V₂ was first determined by filling
187 the sample tube completely with water and weighing it. This yielded V₂ = 19.00 ml ±
188 0.3 ml. V₁ was measured by determining by filling the gas reservoir first with air and
189 then connecting it to the evacuated sample tube. From the initial pressure p₁ in the
190 reservoir and the final pressure p₂ one can calculate V₁ by applying the ideal gas law
191 pV = nRT (with p = pressure, V = Volume, n = number of mols, R = gas constant, and
192 T = temperature) : $V_1 = \frac{p_2 V_2}{p_1 - p_2}$. This yielded V₁ = 617ml ± 6 ml. The free gas volume
193 V₃ in the sample container can be calculated by subtracting the volume of the glass
194 powder from V₂: $V_3 = V_2 - \frac{m_{\text{glass}}}{\rho_{\text{glass}}}$, where m_{glass} and ρ_{glass} are mass and density of the
195 glass powder, respectively. The pressure drop Δp due to adsorption can be readily
196 converted into the number of adsorbed moles Δn, if the ideal gas law is applied:

197
198

$$\Delta n = \Delta p \frac{V_1 + V_3}{RT}$$

199
200 However, while the ideal gas law describes air at 1 bar and lower pressures very well,
201 for SO₂ significant deviations may occur due to non-ideal behavior. Therefore, all
202 calculations for SO₂ were carried out using the van der Waals equation

203

204
$$p = \frac{nRT}{V - b} - \frac{an^2}{V^2}$$

205

206 with the constants $a = 0.69 \text{ Pa m}^6 \text{ mol}^{-2}$ and $b = 5.7 \cdot 10^{-5} \text{ m}^3 \text{ mol}^{-1}$ for SO₂. In order to
207 calculate the number of adsorbed moles of gas from the observed pressure drop, the
208 van der Waals equation was rearranged into a third-order equation in n , which was
209 solved by the Cardano formula. At room temperature and above, the differences
210 between the calculations using ideal gas law and the van der Waals equation are
211 negligible. However, they may amount to a few percent (relative) at 0 °C and below.
212 The van der Waals equation was chosen, because it is well suited to describe non-
213 ideal gases at low pressures. However, as the deviations from ideal gas behavior are
214 small under all conditions studied, very similar results could also have been obtained,
215 e.g. by a virial type equation.

216

217 Uncertainties in the calculated surface concentrations were determined by a full error
218 propagation analysis including the uncertainties of all parameters that enter the
219 calculation. Main sources of uncertainty are the pressures, the volumes in the system
220 and the specific surfaces of the powders.

221

222

223 **EXPERIMENTAL RESULTS**

224

225 **Adsorption experiments at room temperature**

226 Adsorption and desorption isotherms for rhyolite, dacite and andesite glass powders
227 are shown in Fig. 2. The shape of the curve for adsorption, most clearly seen for the
228 dacite sample, corresponds to a “type II” isotherm according to the classification of
229 Brunauer (1945): The amount of adsorbed gas first increases steeply, then reaches a
230 nearly flat plateau until it starts to increase again. This type of curve suggests that
231 adsorption occurs in several layers. The nearly flat part of the curve corresponds

232 approximately to the adsorption of the first layer of gas molecules on the surface.
233 When pressure is reduced, desorption occurs. However, desorption is not fully
234 reversible; rather, some hysteresis-like behavior is obvious from Fig. 2, implying that
235 during adsorption and/or desorption, only some metastable equilibrium is reached.
236 The amount of SO₂ remaining on the surface at very low pressure corresponds
237 approximately to the first layer of gas molecules on the surface, i.e. to the amount of
238 SO₂ adsorbed in the shallow part of the adsorption curve as seen in Fig. 2. In order to
239 confirm that some SO₂ remains irreversibly attached to the surface, the samples were
240 analyzed by X-ray fluorescence (XRF) after the end of the desorption experiment.
241 Bulk SO₂ concentrations of 2381 ± 328 ppm by weight were observed for the rhyolite
242 sample, 1286 ± 97 ppm for the dacite sample and 783 ± 33 ppm for the andesite
243 sample. These values are broadly consistent with the data obtained from the
244 adsorption/desorption data (Table 2). The differences may be related to the handling
245 of the samples in air of about 50 % relative humidity during preparation for XRF
246 analysis, which may have caused some desorption of SO₂ by interaction with air or
247 water vapor. The generally quite high bulk sulfur contents of these samples reflect
248 their small grain size and correspondingly high specific surface. The oxidation state of
249 sulfur on the surfaces of andesite, dacite, and rhyolite glasses exposed to SO₂ gas for
250 24 hours was studied by Farges et al. (2009). From sulfur K-edge XANES data, it
251 appears that most of the sulfur is adsorbed as sulfate, which may have formed by
252 reaction of SO₂ with broken bonds at the glass surface.

253

254 **Adsorption experiments at variable temperature**

255 Adsorption isotherms of SO₂ on rhyolite glass powder are shown in Fig. 3a for
256 variable temperatures, ranging from - 80 °C to + 150°C. Clearly adsorption strongly
257 decreases with temperature. As sulfur dioxide condenses to a liquid already at -10 °C
258 at 1 bar, the low-temperature adsorption experiments could only be carried out up to
259 low pressures. Adsorption measurements on andesite and dacite glass at 0°C and 20°C
260 show a similar increase of adsorption with decreasing temperature as seen for rhyolite
261 (Fig. 3b, c). The decrease of adsorption with increasing temperature is typical for the
262 interaction of gases with surfaces. Since the entropy of SO₂ in the gas phase is higher
263 than on a surface and since the entropy contribution $T\Delta S$ to Gibbs free energy $\Delta G =$

264 $\Delta H - T\Delta S$ (where ΔH is the adsorption enthalpy) increases with temperature, high
265 temperatures shift the equilibrium towards the free gas.

266

267 Measured adsorption data at different temperatures were fitted to BET (Brunauer-
268 Emmet-Teller) adsorption isotherms, which are designed to describe multilayer
269 adsorption (Brunauer et al. 1938):

270

$$271 \quad \frac{p}{V(p_0 - p)} = \frac{1}{V_m C} + \frac{C-1}{V_m C} \left(\frac{p}{p_0} \right)$$

272

273 where p is pressure, V is the volume of the adsorbed gas at STP (standard pressure
274 and temperature), p_0 is the condensation pressure of the gas at the given temperature,
275 V_m is the monolayer capacity, i.e. the volume of gas adsorbed in the first complete
276 layer of gas molecules, where the volume is given at STP conditions, and C is a
277 constant related to the interaction energy between gas molecules and surface. This

278 equation implies that a plot of $\frac{p}{V(p_0 - p)}$ versus $\frac{p}{p_0}$ should yield a straight line with

279 intercept $\frac{1}{V_m C}$ and slope $\frac{C-1}{V_m C}$, which allows the two constants V_m and C to be

280 determined. Bet isotherm plots for rhyolite, dacite and andesite composition at 0°C
281 and 25°C are shown in Fig. 4, the corresponding BET constants are compiled in Table
282 3.

283

284 **Adsorption experiments with natural obsidian glasses**

285 Figure 5 shows adsorption and desorption isotherms measured on powders of natural
286 obsidians from Lipari (Aeolian Islands, Italy; rhyolitic composition) and from Puu
287 Waawaa (Hawaii; trachytic composition) at 0 °C. The data are broadly comparable to
288 those for the synthetic samples (Fig. 3), suggesting that the presence or absence of
289 iron (1.5 wt. % FeO_{tot} for Lipari obsidian and 4.1 wt. % for Puu Waawaa obsidian)
290 does not fundamentally change the absorption behavior. BET constants derived from
291 these data are also included in Table 3.

292

293

294

295 **A multiple regression model of SO₂ adsorption**

296 In order to construct a numerical model for SO₂ adsorption that includes both partial
297 pressure and temperature, the data for each glass composition were fitted to an
298 equation

299

300
$$\ln c = A \frac{1}{T} + B \ln p + C$$

301

302 where c is the amount of adsorbed SO₂ in mg/m² (milligram per m² of surface area), p
303 is SO₂ partial pressure in mbar and T is temperature in Kelvin; A, B, and C are
304 constants obtained by multiple regression. This equation corresponds to a Freundlich
305 adsorption isotherm (Freundlich, 1907) with an added term AT⁻¹ to describe the
306 temperature dependence. The Freundlich isotherm is an empirical equation, which
307 often describes absorption equilibria well; because of its functional simplicity, it is
308 particularly suitable to fit absorption data over a wide range of P and T conditions.

309 The constant A is related to the adsorption enthalpy ΔH by A = - ΔH/R where R is the
310 gas constant. Fit parameters for this equation are given in Table 4; Figure 6 compares
311 predicted and observed surface concentrations of SO₂. The calculated values for the
312 coefficient A correspond to adsorption enthalpies ΔH (in kJ/mol) of - 7.6 ± 1.0 for
313 rhyolite glass, - 17.8 ± 3.1 for dacite glass, and - 13.7 ± 3.0 for andesite glass. The
314 value for dacite glass is close to the - 26 kJ/mol reported for SO₂ adsorption on MCM-
315 41, a mesoporous aluminosilicate material, at high surface coverage (Branton et al.
316 1995).

317

318 **SULFUR ADSORPTION IN VOLCANIC PLUMES**

319 Based on ash leachate data of from the 1974 Fuego eruption, Rose (1977) already
320 suggested that about 33 % of the originally released sulfur was scavenged by ash.

321 With the quantitative adsorption data provided in this study, it is now possible to
322 quantify the extent of SO₂ scavenging by ashes and its dependence on eruption
323 parameters. In this context, the most important results of this study are:

324

325 (1) SO₂ adsorption strongly decreases with temperature; therefore, probably most of
326 the adsorption occurs in the cold parts of the plume higher in the atmosphere, while
327 adsorption at magmatic temperatures is likely of minor importance. The short

328 residence time of particles at near-vent conditions in explosive eruptions (a few
329 minutes at most) as opposed to the long residence time in the umbrella part of a plume
330 (hours to days) also suggest that most adsorption must occur at low temperature. This
331 is entirely consistent with the observation by Bagnato et al. (2013) that the sulfur load
332 on ash surfaces of the 2010 Eyafjallajökull eruption increased by more than a factor of
333 three with increasing residence time and distance from the vent.

334

335 (2) The coefficient B in the multiple regression equations (Table 4) suggest that SO₂
336 adsorption increases only slightly with the partial pressure of SO₂, i.e. with p^{0.2} to p^{0.3}.
337 In other words, SO₂ adsorption remains strong at very low partial pressures, again
338 confirming that adsorption occurs mostly in the dilute and cold parts of plumes.
339 Moreover, while the amount of adsorbed SO₂ increases only with p^{0.2} - p^{0.3}, the
340 amount of SO₂ remaining in the gas phase is directly proportional to the SO₂ partial
341 pressure p. Therefore, the fraction of total SO₂ that is not adsorbed must increase with
342 $p/p^{0.3} = p^{3.3}$ or $p/p^{0.2} = p^5$. This means that the initial SO₂ partial pressure, i.e. the
343 molar fraction of SO₂ in the volcanic gases exerts a major control on the extent of SO₂
344 adsorption, together with the ratio of ash surface to total gas volume.

345

346 (3) The first monolayer of SO₂ on ash surfaces appears to be irreversibly adsorbed,
347 implying that this part of SO₂ is permanently removed from the plume. SO₂ that is
348 adsorbed in multiple layers may be released again during desorption, when the SO₂
349 partial pressure is reduced, e.g. upon dilution of the plume by entrainment of air. The
350 data in Fig. 2 suggest that the amount of SO₂ that may be irreversibly adsorbed on ash
351 surfaces is close to 0.8 to 1 mg/m². Interestingly, the data of Bagnato et al. (2013;
352 their Fig. 15c) suggest that at residence times of ashes in the plume of 1 hour and
353 above, sulfur concentrations on the ashes level out at 1.2 mg/m² of sulfate, which
354 converts to 0.9 mg/m² of SO₂, in very good agreement with the experimental data
355 reported here.

356

357 (4) Glass composition has only a relatively minor effect on the extent of SO₂
358 adsorption on ash surfaces. The differences between the data for rhyolite, dacite and
359 andesite glass (Fig. 2) are mostly below 25 % (relative), which is negligible compared
360 to the much stronger effects of pressure and temperature (Fig. 3.).

361

362 The experimental data presented here were all obtained by equilibrating ash surfaces
363 with pure SO₂ gas, while in nature, the gas phase will be a mixture of volcanic gases
364 and air. The main component of the volcanic gases is usually H₂O, followed by CO₂,
365 SO₂ and HCl. SO₂ is typically in the range of up to a few mole %, with HCl usually
366 being somewhat less abundant (Symonds et al. 1996). In the cold parts of a volcanic
367 plume, these gases are highly diluted by mixing with air, which reduces potential
368 interactions between the gases by competition for adsorption sites. In particular for
369 HCl, the concentration in the plume is strongly reduced, due to the high solubility of
370 HCl in liquid water and its incorporation into ice (Textor et al. 2003; Rose et al.
371 2006). Because of the very low HCl partial pressures resulting, interaction between
372 HCl and SO₂ in the adsorption process on ashes can likely be ignored. Water vapor,
373 however, will be much more abundant than SO₂, both in the initial volcanic gases and
374 in the diluted plume. This will even be so for initially CO₂-rich volcanic gases,
375 because of the extensive mixing with (humid) air (see the discussion of dilution
376 factors below). During the preparation of the samples used in this study, direct
377 contact with liquid water during grinding was avoided, as this would very likely have
378 caused some change in surface properties due to leaching. However, the powder
379 samples were handled in air of average humidity and several studies have shown that
380 any silicate surface exposed to air of normal humidity will immediately be coated by
381 water molecules, which will not be removed even in vacuum, unless the sample is
382 heated to temperatures far above 100 °C (Kunkel 1950; Nelson and Vey 1968;
383 Zhuravlev 1987; Garofalini 1990; see also Keppler and Rauch 2000; Lathem et al.
384 2011). Measurement of the adsorption of water vapor on silicate glass (Razouk and
385 Salem 1948) show that it can be described by a type II isotherm, very similar in shape
386 to those measured for SO₂ in this study. Already at relative humidities of < 10 %, the
387 surface of the glass is nearly completely covered by water molecules and the isotherm
388 remains nearly flat (i.e. not much additional adsorption occurs) up to very high
389 relative humidities of > 70 %. Therefore, the samples investigated in this study likely
390 had surfaces initially coated by water molecules and the adsorption measurements are
391 entirely realistic for the processes that occur in dilute volcanic plumes at high altitude.
392
393 To illustrate the effect of ashes on the SO₂ yield of explosive eruptions, we use our
394 data to simulate the behavior of SO₂ in a plume. For quantitative calculations, the
395 following factors have to be considered:

396

397 (1) Available ash surface. The 1980 Mt. St Helens eruption produced ash with a
398 median grain size around 10 μm (Carey and Sigurdsson 1982; Genarau et al. 2012).
399 Assuming a uniform grain size of 10 μm , a cubic shape of individual grains and a
400 density of 2.4 g/cm^3 , yields a specific surface of the ash of 250 m^2/kg . This is quite
401 comparable to specific ash surfaces measured for the 2010 Eyafjallajökull eruption
402 (Bagnato et al. 2013). For comparison, we will also discuss the situation for ashes
403 with a grain size of 1 μm , and a specific surface of 2500 m^2/kg , similar to the powders
404 used in our experiments. While this size appears small compared to measured grain
405 size distributions of ashes, it has to be kept in mind that these measurements are
406 usually carried out on ashes that have sedimented out of the plume within a few hours
407 or days. The grain size of ash deposits often decreases exponentially with distance
408 from the vent. Very fine particles will remain in the plume for longer times and may
409 therefore be under-represented in the sampling (Pyle 1989, Bonadonna and Houghton
410 2005). Using satellite data, Wen and Rose (1994) estimated an average particle size of
411 2 – 2.5 μm in the ash cloud of the 1992 eruption of Crater Peak/Spurr Volcano. This
412 would be similar for the finest grain sizes used in our experiments. On the other hand,
413 Bonadonna et al. (2011) report a median near 250 μm for the total grain size
414 distribution of the 2010 Eyafjallajökull eruption, with a fine-ash content of 30 wt. %.
415 Note, however, that the fine ash particles contribute much more strongly to the
416 average specific surface than large particles and therefore, the specific surface of the
417 ash will be mostly determined by the abundance of very fine particles.

418

419 (2) Temperature. Many plumes from explosive eruptions reach the stratosphere and
420 spread there horizontally. Due to extensive mixing with air and conductive heat loss,
421 the temperature of the plume gases will be similar to the ambient temperature (e.g.
422 Sparks 1997; Textor et al. 2003, 2006), which is approximately 220 K (-53 °C) at 10
423 km altitude. We will assume this temperature for all our calculations.

424

425 (3) Mass ratio of sulfur dioxide to ash. This ratio is determined by the composition of
426 the volcanic gases and by the mass ratio of gas to ash. Measured SO_2 contents in
427 volcanic gases vary widely, between < 1 mole % to > 10 mole % (Symonds et al.
428 1994), where 1 mole % corresponds to 3.47 wt. % in a gas phase consisting mostly of

429 water vapor. This wide variation may partially be due to the strong partitioning of SO₂
430 into the vapor phase in equilibrium with a silicate melt (e.g. Keppler 2010 and
431 references therein), implying that SO₂ will be highly enriched in the initial fluids
432 released at the beginning of an eruption and depleted during further degassing. For the
433 1991 Mt. Pinatubo eruption, an SO₂ concentration in the pre-eruptive fluid phase
434 between 0.56 and 0.85 wt. % was estimated (Keppler 1999), i.e. the gas released by
435 this eruption was not particularly sulfur-rich, but the mass ratio of pre-eruptive fluid
436 to magma (0.08 – 0.25; Keppler 1999) was very high. For the weight ratio of total
437 volcanic gases to (glassy) ash we will here assume a value of 0.05, i.e. the mass of the
438 gases released is 5 % of the mass of the magma. This assumption is in line with the
439 pre-eruptive volatile (mostly water) contents of mafic arc magmas, which usually
440 cluster between 2 and 6 wt. % (Métrich and Wallace, 2008; Plank et al. 2013);
441 somewhat higher volatile concentrations may be reached in more evolved magmas.
442

443 (4) Partial pressure of SO₂ in the plume. Compared to the partial pressure in the initial
444 volcanic gases, the partial pressure in the plume will be reduced by the decrease of
445 ambient pressure and by the mixing with air. At an elevation of 10 km, ambient
446 pressure decreases from about 1 bar near sea level to about 200 mbar. This effect
447 alone would therefore reduce the partial pressure of 1 mole % SO₂ in a volcanic gas
448 from 10 mbar to 2 mbar, assuming ideal gas behavior, which is a very good
449 approximation at these low pressures. The degree of mixing with air depends on
450 various physical parameters of the eruption. We will assume a dilution of the volcanic
451 gas by air by a factor of 100:1 in our calculations, which is a plausible value for a
452 range of parameters (initial temperatures around 1000 K, entrainment coefficients ϵ
453 around 0.09 and a weight ratio of volcanic gases to ash of 0.05; for discussion, see
454 Sparks et al. 1997; Schmauss-Schreiner 2007). In the given example, this will reduce
455 the SO₂ partial pressure to 0.02 mbar. We note, however, that the extent of adsorption
456 is rather insensitive to this parameter, as absorption only increases with $p^{0.2}$ - $p^{0.3}$.
457 Therefore, increasing the dilution factor of the plume from 100 to 1000 would only
458 reduce the amount of adsorbed SO₂ by a factor of 1.5 – 2.

459

460 If one assumes a specific surface of the volcanic ash of 250 m²/kg, a mass ratio of
461 gas/ash of 0.05 as discussed above and 1 mole % of SO₂ in the gas, complete

462 adsorption of SO₂ on the ash surface would yield a surface concentration of 6.94
463 mg/m². A comparison with the data in Figure 2c and 3 shows that this values is at
464 least three times higher than the highest surface concentration measured, even at very
465 high SO₂ partial pressures which likely will never be reached in a plume. Therefore,
466 even under the most favorable circumstances, not more than about 30 % of the total
467 SO₂ in the plume could be absorbed by ash, the real fraction likely being lower. This
468 fraction will decrease further, if the initial SO₂ concentration in the volcanic gas is
469 higher than 1 mol %, because the amount of absorbed SO₂ only increases with $p^{0.2} - p$
470 $^{0.3}$. On the other hand, if one assumes a specific surface of the ash of 2500 m²/kg, at 1
471 mol % of SO₂ in the gas, total absorption would lead to a surface concentration of
472 0.69 mg/m², which is well in the range of values that may be achieved at very low
473 partial pressures of SO₂ (Fig. 2 and 3), so that removal of most of the SO₂ from the
474 plume may be possible. Already these simple considerations show that (1) nearly
475 complete loss of SO₂ from a plume by adsorption may be possible, if the initial SO₂
476 concentration is far below 1 mole % and /or the ash is very fine-grained; (2) for initial
477 SO₂ concentrations of 1 mole % or higher, most of the SO₂ will likely remain in the
478 gas phase of the plume.

479

480 For a quantitative modeling of SO₂ adsorption, the adsorption isotherm at plume
481 temperatures (220 K) has to be calculated from the fit parameters in Table 4. This
482 isotherm is shown in Figure 7 for andesite glass. For 1 mole % SO₂ in the volcanic
483 gas, the SO₂ partial pressure in the plume before adsorption will be 0.02 mbar. For
484 andesite glass with a very large surface (specific surface 2500 m²/kg, mass ratio
485 gas/ash = 0.05), this partial pressure corresponds to a surface concentration of SO₂ of
486 0.34 mg/m². However, this is not the equilibrium surface concentration, because the
487 SO₂ partial pressure in the gas decreases as SO₂ is being absorbed. The equilibrium
488 surface concentration for a given initial SO₂ partial pressure can be obtained by a
489 graphical method (Fig. 7). The initial state of the system corresponds to a surface
490 concentration of SO₂ of zero and a SO₂ partial pressure of 0.02 mbar. This state is
491 marked as point A in Figure 7. Total absorption of all SO₂ (resulting in zero partial
492 pressure) would lead to a surface concentration of 0.69 mg/m²; this is point B in Fig.
493 7. As absorption proceeds, the increase in surface concentrations has to be
494 proportional to the decrease in partial pressure of SO₂, as both quantities are
495 proportional to the numbers of absorbed moles of SO₂. Therefore, in the diagram

496 shown in Figure 7, the system has to move along a straight line from point A in the
497 direction towards point B during the adsorption process, until adsorption stops
498 because equilibrium is reached. This point is given by the intersection of the straight
499 line with the adsorption isotherm, which relates the surface concentration to the SO₂
500 partial pressure in equilibrium. In the present example, the surface concentration is
501 0.29 mg/m², with an equilibrium SO₂ partial pressure of 0.012 mbar. This implies that
502 42 % of the SO₂ initially released by the eruption was scavenged by ash. The latter
503 number is obtained as the ratio of the equilibrium surface concentration to the
504 (hypothetical) surface concentration corresponding to total absorption (0.69 mg/m²).
505 This percentage can also be obtained graphically; in Figure 7, it is the ratio of the
506 distance between the equilibrium point and point A to the distance between A and B.
507

508 Figure 8 shows model calculations for the fraction of SO₂ in a plume adsorbed on
509 ashes, for two different specific ash surfaces and for variable SO₂ contents in the
510 volcanic gas. Obviously, SO₂ absorption can be very important if the ash surface is
511 high and if the initial SO₂ content of the volcanic gas is below 1 mole %. All
512 calculations were carried out for a mass ratio of volcanic gas to ash of 0.05. However,
513 the result of the calculations does not change, if the product of the mole fraction of
514 SO₂ in the volcanic gas and the mass ratio of gas/ash remains constant. In other
515 words, for a gas/ash mass ratio of 0.1 and an SO₂ content of 1 mole %, the fraction of
516 SO₂ adsorbed on ash is the same as for a gas/ash mass ratio of 0.05 and 2 mole %
517 SO₂.

518
519 Our data give first insights into the initial adsorption processes occurring in volcanic
520 plumes at high altitude. Subsequent to the adsorption of SO₂ and other gases on ash
521 particles, surface reactions may occur that involve the leaching of cations out of the
522 ash and the re-precipitation of salts on the ash surface (e.g. Delmelle et al. 2007;
523 Bagnato et al. 2013). Very likely, however, these processes require the presence of
524 liquid water and therefore, they only occur when ash particles started to sediment
525 down to warmer parts of the atmosphere.

526
527 According to the results presented here, adsorption may under some circumstances
528 strongly affect the sulfur yield of eruptions and by implication, their impact on
529 climate. Clearly, both the relative amount of available ash surface (as controlled by

530 the gas mass fraction and the grain size or specific surface of the ash) and the initial
531 SO₂ concentration in the gases are critical parameters. If SO₂ is very diluted, e.g. by
532 water vapor in the volcanic gas, it may be largely adsorbed by the volcanic ash and
533 the environmental impact of such an eruption is like to be small. On the other hand if
534 the initial SO₂ concentration in the volcanic gas, or the ratio of volcanic gas to ash is
535 high, only a much smaller fraction of SO₂ will be adsorbed and a much stronger
536 impact on climate is to be expected. The 1991 Mt. Pinatubo eruption may have been
537 such a case; Guo et al. (2004) used infrared remote sensing data from satellites to
538 infer that the cloud initially contained 50 Mt of ash particles, but up to 12 Mt of SO₂.
539 From the data presented in this study, it is clear that sulfur scavenging by ash is
540 insignificant under such circumstances.

541

542 If one compares two eruptions that release the same total amount of SO₂, the one
543 releasing more water vapor will be more explosive. However, the dilution of SO₂ by
544 water vapor will also enhance adsorption of SO₂ on ash and therefore, the more
545 explosive eruption may have a smaller impact on climate. This effect is further
546 enhanced by the stronger fragmentation and therefore larger ash surface resulting
547 from a more explosive eruption. SO₂ adsorption on ashes may therefore be a decisive
548 factor in controlling the environmental impact of volcanic eruptions. In particular, it
549 may be one of the reasons why atmospheric cooling does not always correlate with
550 the magnitude of an eruption or with total sulfur yield.

551

552

553

IMPLICATIONS

554 The model for SO₂ adsorption described here allows the scavenging effect of volcanic
555 ashes on the SO₂ abundance in volcanic plumes to be fully quantified, such that this
556 effect can now be incorporated in numerical models of plume chemistry. The example
557 calculations shown in this paper cannot explore the full range of parameters that may
558 occur in plumes. However, they suggest that the relative amount of available ash
559 surface and the initial concentration of SO₂ in the volcanic gases are the most
560 important parameters in controlling the extent of adsorption. If the initial SO₂
561 concentration is low (< 1 mole %) and the specific surface area of the ash is high,
562 most of the SO₂ may be adsorbed. This is because adsorption only increases with $p^{0.2}$
563 $- p^{0.3}$, where p is SO₂ partial pressure and therefore, the fraction of SO₂ in the plume

564 that is not adsorbed on ash must increase with $p^{3.3}$ to p^5 . As SO_2 adsorption on
565 volcanic ash may under some circumstances greatly reduce the effect of volcanic
566 eruptions on climate, the model presented in this study should allow a significant
567 improvement in forecasting the environmental impact of volcanic eruptions.

568

569

570

ACKNOWLEDGEMENTS

571

572 This work was supported by German Science Foundation (DFG; Leibniz Award to
573 H.K.). We thank Christoph Berthold, University of Tübingen, for his help during the
574 early stages of this study. Constructive reviews by Malcolm Rutherford, Don Baker
575 and an anonymous referee helped to improve the manuscript.

576

577

578

REFERENCES CITED

- 579 Ayris, P.M., Lee, A.F., Wilson, K., Kueppers, U., Dingwell D.B., and Delmelle, P.
580 (2013) SO_2 sequestration in large volcanic eruptions: High-temperature
581 scavenging by tephra. *Geochimica et Cosmochimica Acta*, 110, 58-69.
- 582 Bagnato, E., Aiuppa, A., Andronico, D., Cristaldi, A., Liotta, M., Brusca, L., and
583 Miraglia, L. (2011) Leachate analyses of volcanic ashes from Stromboli volcano:
584 A proxy for the volcanic gas plume composition? *Journal of Geophysical*
585 *Research*, 116, D17204, DOI: 10.1029/2010JD015512.
- 586 Bagnato, E., Aiuppa, A., Bertagnini, A., Bonadonna, C., Cioni, R., Pistolesi, M.,
587 Pedone, M., and Hoskuldson, A. (2013) Scavenging of sulphur, halogens and
588 trace metals by volcanic ash: The 2010 Eyafjallajökull eruption. *Geochimica et*
589 *Cosmochimica Acta*, 103, 138-160.
- 590 Bekki, S. (1995) Oxidation of volcanic SO_2 : a sink for stratospheric OH and H_2O .
591 *Geophysical Research Letters*, 22, 913-916.
- 592 Binder, B. and Keppler, H. (2011) The oxidation state of sulfur in magmatic fluids.
593 *Earth and Planetary Science Letters*, 301, 190-198.
- 594 Bluth, G. J. S., Schnetzler, C. C., Krueger, A. J., and Walter, L. S. (1993) The
595 contribution of explosive volcanism to global atmospheric sulfur-dioxide
596 concentrations. *Nature*, 366, 327-329.

- 597 Bonadonna, C. and Houghton, B.F. (2005) Total grain-size distribution and volume of
598 tephra-fall deposits. *Bulletin of Volcanology*, 67, 441-456.
- 599 Bonadonna, C., Genco, R., Gouhier, M., Pistolesi, M., Cioni, R., Alfano, F.,
600 Hoskuldsson, A., and Ripepe, M. (2011) Tephra sedimentation during the 2010
601 Eyjafjallajökull eruption (Iceland) from deposit, radar, and satellite observations.
602 *Journal of Geophysical Research*, 116, Article number B12202,
603 doi:10.1029/2011JB008462.
- 604 Branton, P.J., Hall, P.G., Treguer, M., and Sing, K.S.W. (1995) Adsorption of carbon
605 dioxide, sulfur dioxide and water vapour by MCM-41, a model mesoporous
606 adsorbent. *Journal of the Chemical Society – Faraday Transactions*, 91, 2041-
607 2043.
- 608 Briffa, K. R., Jones, P. D., Schweingruber, F. H., and Osborn, T. J. (1998) Influence
609 of volcanic eruptions on Northern Hemisphere summer temperatures over the
610 past 600 years. *Nature*, 393, 450-454.
- 611 Brunauer, S. (1945) *The adsorption of gases and vapors*, vol. 1. Princeton University
612 Press.
- 613 Brunauer, S., Emmet, P. H., and Teller, E. (1938) Adsorption of gases in
614 multimolecular layers. *Journal of the American Chemical Society*, 60, 309-319.
- 615 Carey, S. N. and Sigurdsson, H. (1982) Influence of particle aggregation on
616 deposition of distal tephra from the May 18, 1980 eruption of Mount St. Helens
617 volcano. *Journal of Geophysical Research*, 87, 7061-7062.
- 618 Delmelle, P., Lambert, M., Dufrene, Y., Gerin, P., and Oskarsson, N. (2007)
619 Gas/aerosol-ash interaction in volcanic plumes: New insights from surface
620 analyses of fine ash particles. *Earth and Planetary Science Letters*, 259, 159-170.
- 621 de Silva, S. L. and Zielinski, G. A. (1998) Global influence of the AD 1600 eruption
622 of Huaynaputina, Peru. *Nature*, 393, 455-458.
- 623 Farges, F., Keppler, H., Flank, A.-M., and Lagarde, P. (2009) Sulfur K-edge XANES
624 study of S sorbed onto volcanic ashes. *Journal of Physics: Conference Series*,
625 190, 012177.
- 626 Freundlich, H. (1907) Über die Adsorption in Lösungen. *Zeitschrift für physikalische*
627 *Chemie*, 57, 385-470.
- 628 Frogner, P., Gislason, S. R., and Oskarsson, N. (2001) Fertilizing potential of volcanic
629 ash in ocean surface water. *Geology*, 29, 487-490.

- 630 Garofalini, S.H. (1990) Molecular dynamics computer simulations of silica surface
631 structure and adsorption of water molecules. *Journal of Non-Crystalline Solids*,
632 120, 1-12.
- 633 Genareau, K., Proussevitch, A.A., Durant, A.J., Mulukutla, G., and Sahagian, D.L.
634 (2012) Sizing up the bubbles that produce very fine ash during explosive volcanic
635 eruptions. *Geophysical Research Letters*, 39, L15306,
636 doi:10.1029/2012GL052471.
- 637 Gu, Y, Gierke, J. S., Bluth, G. J., and Rose, W. I. (1999) A laboratory study of sulfur
638 dioxide adsorption onto fine dacitic volcanic ash. *EOS, Transactions of the*
639 *American Geophysical Union* 80, F135 (Fall Meeting Abstracts).
- 640 Guffanti, M., Schneider, D.J., Wallace, K.L., Hall, T., Bensimon, D.R., and Salinas,
641 L.J. (2010) Aviation response to a widely dispersed volcanic ash and gas cloud
642 from the August 2008 eruption of Kasatochi, Alaska, USA. *Journal of*
643 *Geophysical Research*, 115, D00L19, DOI: 10.1029/2010JD013868.
- 644 Guo, S., Rose, W.I., Bluth, G.J.S., and Watson, I.M. (2004) Particles in the great
645 Pinatubo volcanic cloud of June 1991: The role of ice. *Geochemistry,*
646 *Geophysics, Geosystems*, 5, Article number Q05003,
647 doi:10.1029/2003GC000655.
- 648 Jones, M.T. and Gislason, S.R. (2008) Rapid releases of metal salts and nutrients
649 following the deposition of volcanic ash into aqueous environments. *Geochimica*
650 *et Cosmochimica Acta*, 72, 3661-3680.
- 651 Jordan, A., Harnisch, J., Borchers, R., Le Guern, F.N., and Shinohara, H. (2000)
652 Volcanogenic halocarbons. *Environmental Science & Technology*, 34, 1122-
653 1124.
- 654 Keppler, H. (1999) Experimental evidence for the source of excess sulfur in explosive
655 volcanic eruptions. *Science*, 284, 1652-1654.
- 656 Keppler, H. (2010) The distribution of sulfur between haplogranitic melts and
657 aqueous fluids. *Geochimica et Cosmochimica Acta*, 74, 645-660.
- 658 Keppler, H. and Rauch, M. (2000) Water solubility in nominally anhydrous minerals
659 measured by FTIR and ¹H MAS NMR: the effect of sample preparation. *Physics*
660 *and Chemistry of Minerals*, 27, 371-376.
- 661 Krotkov, NA, Schoeberl, MR, Morris, GA, Carn, S, Yang, K (2010) Dispersion and
662 lifetime of the SO₂ cloud from the August 2008 Kasatochi eruption. *Journal of*

- 663 Geophysical Research-Atmospheres, 115, Article Number: D00L20, DOI:
664 10.1029/2010JD013984.
- 665 Kunkel, W.B. (1950) The static electrification of dust particles on dispersion into a
666 cloud. *Journal of Applied Physics*, 21, 820-832.
- 667 Lathem, T.L., Kumar, P., Nenes, A., Dufek, J., Sokolik, I.N., Trail, M., and Russel, A.
668 (2011) Hygroscopic properties of volcanic ash. *Geophysical Research Letters*, 38,
669 L11802, doi:10.1029/2011GL047298.
- 670 Leed, E.A. and Pantano, C.G. (2003) Computer modeling of water adsorption on
671 silica and silicate glass fracture surfaces. *Journal of non-crystalline solids*, 325,
672 48-60.
- 673 Mather, T. A. (2008) Volcanism and the atmosphere: the potential role of the
674 atmosphere in unlocking the reactivity of volcanic emissions. *Transactions of the*
675 *Royal Society, A* 366, 4581-4595.
- 676 McCormick, M. P., Thomason, L. W., and Trepte, C. R. (1995) Atmospheric effects
677 of the Mt. Pinatubo eruption. *Nature*, 373, 399-404.
- 678 Métrich, N. and Wallace, P.J. (2008) Volatile abundances in basaltic magmas and
679 their degassing paths tracked by melt inclusions. *Reviews in Mineralogy and*
680 *Geochemistry*, 69, 363-402.
- 681 Nelson, J.D. and Vey, E. (1968) Relative cleanliness as a measure of lunar soil
682 strength. *Journal of Geophysical Research*, 73, 3747-3764.
- 683 Ni, H. and Keppler, H. (2012) In-situ Raman spectroscopic study of sulfur speciation
684 in oxidized magmatic-hydrothermal fluids. *American Mineralogist*, 97, 1348-
685 1353.
- 686 Oskarsson, N. (1980) The interaction between volcanic gases and tephra: fluorine
687 adhering to tephra of the 1970 Hekla eruption. *Journal of Volcanology and*
688 *Geothermal Research*, 8, 251-266.
- 689 Plank, T, Kelley, K.A., Zimmer, M.M., Hauri, E.H., and Wallace, P.J. (2013) Why do
690 mafic arc magmas contain similar to 4 wt% water on average? *Earth and*
691 *Planetary Science Letters*, 364, 168-179.
- 692 Pyle, D.M. (1989) The thickness, volume and grainsize of tephra fall deposits.
693 *Bulletin of Volcanology*, 51, 1-15.
- 694 Razouk, R.I. and Salem, A.S. (1948) The adsorption of water vapor on glass surfaces.
695 *Journal of Physical Chemistry*, 52, 1208-1227.

- 696 Rendulic, K.D. (1988) The influence of surface defects on adsorption and desorption.
697 Applied Physics A, 47, 55-62.
- 698 Robock, A. (2000) Volcanic eruptions and climate. Reviews of Geophysics, 38, 191-
699 219.
- 700 Robock, A., Ammann, C.M., Oman, L., Shindell, D., Levis, S., and Stenchikov, G.
701 (2009) Did the Toba volcanic eruption ~ 74 ka B. P. produce widespread
702 glaciation? Journal of Geophysical Research, 114, D 10107.
- 703 Rodriguez, L.A., Watson, I.M., Edmonds, M., Ryan, G., Hards, V., Oppenheimer,
704 C.M.M., Bluth, G.J.S. (2008) SO₂ loss rates in the plume emitted by Soufriere
705 Hills volcano, Montserrat. Journal of Volcanology and Geothermal Research,
706 173, 135-147.
- 707 Rose, W. I. (1977) Scavenging of volcanic aerosols by ash: atmospheric and
708 volcanologic implications. Geology, 5, 621-624.
- 709 Rose, W.I., Millard, G.A., Mather, T.A., Hunton, D.E., Anderson, B., Oppenheimer,
710 C., Thornton, B.F., Gerlach, T.M., Viggiano, A.A., Kondo, Y., Miller, T.M., and
711 Ballenthin, J.O. (2006) Atmospheric chemistry of a 33-34 hour old volcanic
712 cloud from Hekla Volcano (Iceland): Insights from direct sampling and the
713 application of chemical box modeling. Journal of Geophysical Research, 111,
714 D20206 DOI: 10.1029/2005JD006872.
- 715 Schmauss-Schreiner, D. (2007) Experimental studies on the adsorption of SO₂ on
716 volcanic ashes. Ph. D. thesis, University of Bayreuth, [http://opus.ub.uni-](http://opus.ub.uni-bayreuth.de/volltexte/2008/394/)
717 [bayreuth.de/volltexte/2008/394/](http://opus.ub.uni-bayreuth.de/volltexte/2008/394/).
- 718 Sparks, R. S. J., Bursik, M. I., Carey, S. N., Gilbert, J. S., Glaze, L. S., Sigurdsson, H.,
719 and Woods, A. W. (1997). Volcanic Plumes. John Wiley and Sons.
- 720 Symonds, R.B., Rose, W.I., Bluth, G.J.S., and Gerlach, T.M. (1994) Volcanic-gas
721 studies: Methods, results, and applications. Reviews in Mineralogy, 30, 1-66.
- 722 Textor, C., Graf, H.F., Herzog, M., and Oberhuber, J.M. (2003) Injection of gases into
723 the stratosphere by explosive volcanic eruptions. Journal of Geophysical
724 Research, 108, 4606, DOI: 10.1029/2002JD002987.
- 725 Textor, C., Graf, H.F., Herzog, M., Oberhuber, J.M., Rose, W.I., and Ernst, G.G.J.
726 (2006) Volcanic particle aggregation in explosive eruption columns. Part II:
727 Numerical experiments. Journal of Volcanology and Geothermal Research, 150,
728 378-394.

- 729 Wen, S.M. and Rose, W.I. (1994) Retrieval of sizes and total masses of particles in
730 volcanic clouds using AVHRR bands 4 and 5. *Journal of Geophysical Research –*
731 *Atmospheres*, 99, 5421-5431.
- 732 Witham, C. S., Oppenheimer, C., and Horwell, C. J. (2005) Volcanic ash-leachates: a
733 review and recommendations for sampling methods. *Journal of Volcanology and*
734 *Geothermal Research*, 141, 299-326.
- 735 Zhuravlev, L.T. (1987) Concentration of hydroxyl groups on the surface of
736 amorphous silicas. *Langmuir*, 3, 316-318.

737 **Table 1.** Bulk chemical composition (in wt. %) and density (in g/cm³) of
 738 synthetic glasses

	SiO ₂	Al ₂ O ₃	MgO	CaO	Na ₂ O	K ₂ O	Density
Andesite	56.42	20.81	7.07	7.05	3.68	1.74	2.34
Dacite	67.52	16.25	5.24	2.78	4.29	3.16	2.63
Rhyolite	77.21	12.13	3.08	0.72	2.80	3.46	2.36

739 *Notes:* Chemical composition from XRF, density from pycnometer measurements

740

741

742 **Table 2.** Amount of SO₂ adsorbed on glass powders at 1 bar and amount of SO₂
 743 remaining on the glass surface after desorption. All data for 25 °C.

744

	Adsorbed SO ₂		Pressure
	in mg/m ²	in wt. %	mbar
Rhyolite	1.64 ± 0.32	0.39 ± 0.04	940
Dacite	1.30 ± 0.18	0.41 ± 0.03	968
Andesite	1.30 ± 0.22	0.34 ± 0.03	965
	SO ₂ after desorption		Pressure
	in mg/m ²	in wt. %	mbar
Rhyolite	0.94 ± 0.23	0.22 ± 0.05	6.8
Dacite	0.63 ± 0.16	0.19 ± 0.04	0.9
Andesite	0.75 ± 0.23	0.19 ± 0.04	0.1

745

746

747

748

749

750

751

752

753

754

755

756 **Table 3.** BET fit parameters for the adsorption of SO₂ on glasses.

	T in °C	C	V _m in cm ³ /m ²	R ²
Rhyolite	25	13.1 ± 3.0	0.40 ± 0.08	0.86
	0	93.4 ± 4.7	0.32 ± 0.06	0.99
Dacite	25	19.6 ± 1.0	0.29 ± 0.03	0.97
	0	65.9 ± 3.3	0.34 ± 0.04	0.98
Andesite	25	14.8 ± 3.8	0.40 ± 0.07	0.82
	0	72.0 ± 3.6	0.29 ± 0.05	0.99
Lipari obsidian	0	16.00 ± 0.8	0.33 ± 0.02	0.99
Puu Waawaa obsidian	0	20.10 ± 1.0	0.47 ± 0.02	0.98

757

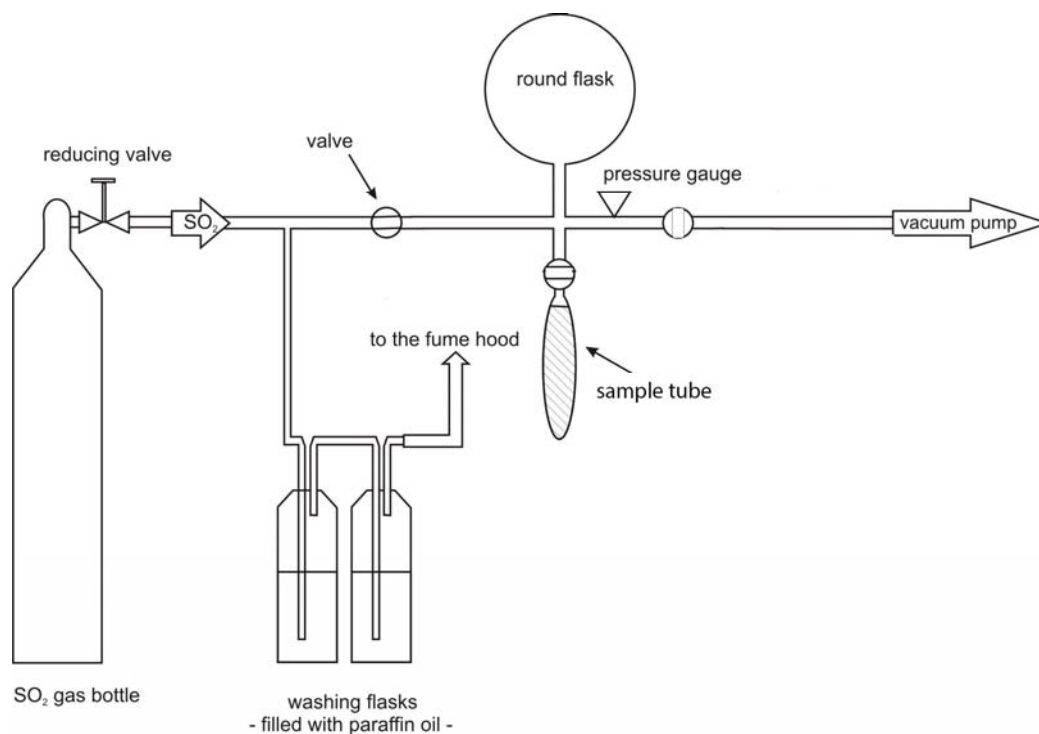
758

759 **Table 4.** Multiple regression coefficients for SO₂ adsorption on rhyolite, dacite and
 760 andesite glasses. Data were fitted to the equation $\ln c = A/T + B \ln p + C$,
 761 where c is the surface concentration of adsorbed SO₂ in mg/m², p is SO₂
 762 partial pressure in mbar and T is temperature in Kelvin.

763

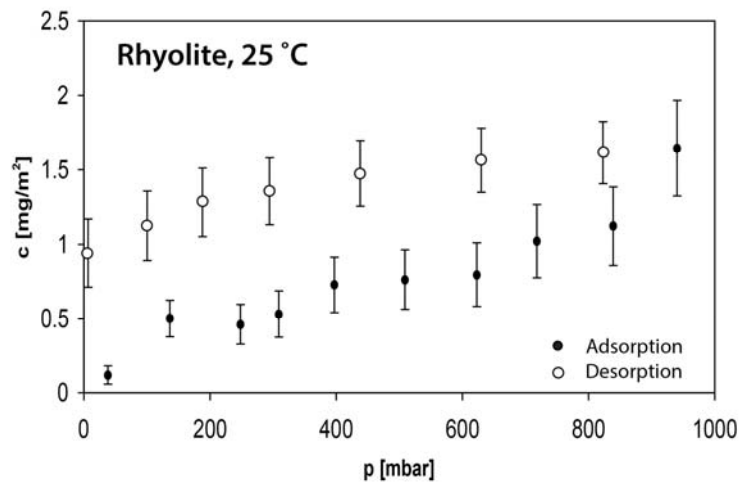
	A	B	C	R ²	Error in ln c
Andesite	1645 ± 363	0.29 ± 0.02	-7.43 ± 1.33	0.92	0.22
Dacite	2140 ± 379	0.29 ± 0.02	-9.32 ± 1.41	0.91	0.20
Rhyolite	910 ± 124	0.21 ± 0.03	-4.48 ± 0.49	0.75	0.37

764

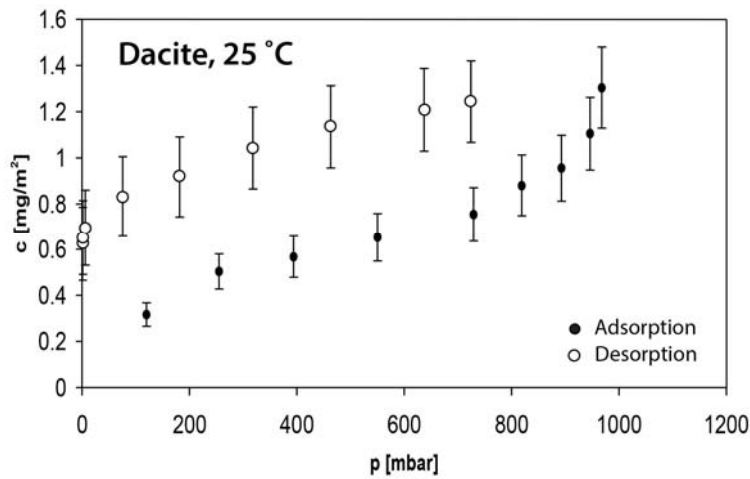


765
766

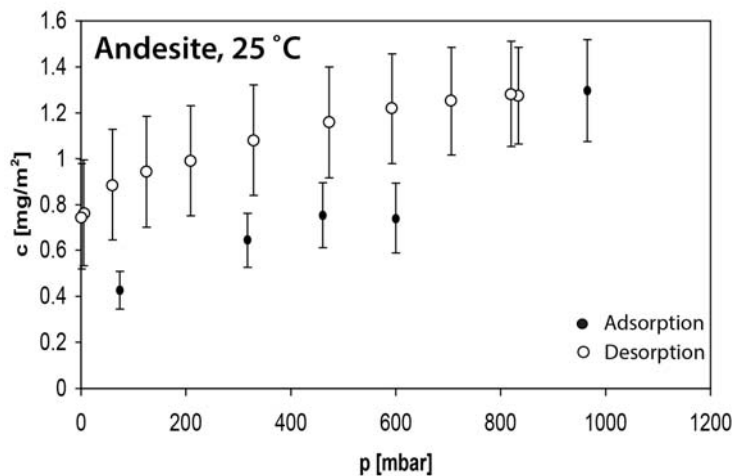
767 **FIGURE 1.** Apparatus used for adsorption measurements. SO₂ is stored in the round
768 glass flask, the powdered ash sample is in the sample tube. When the valve between
769 sample and SO₂ reservoir is opened, the pressure drops due to adsorption of SO₂ on
770 the sample surface. The amount of adsorbed SO₂ can be calculated from the
771 magnitude of the pressure drop.



772

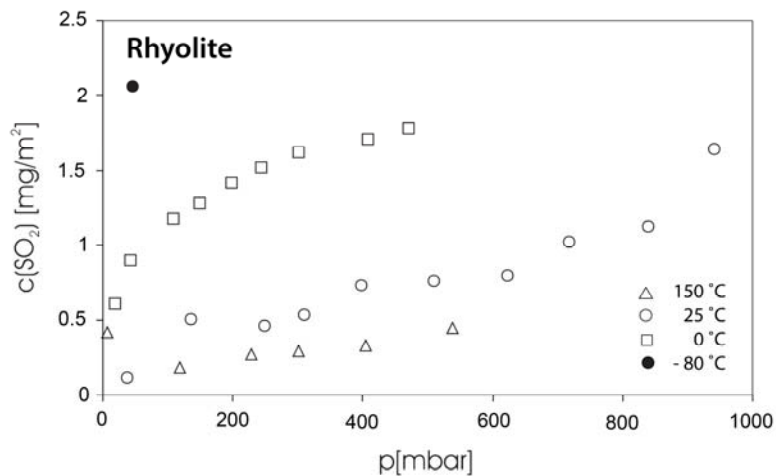


773

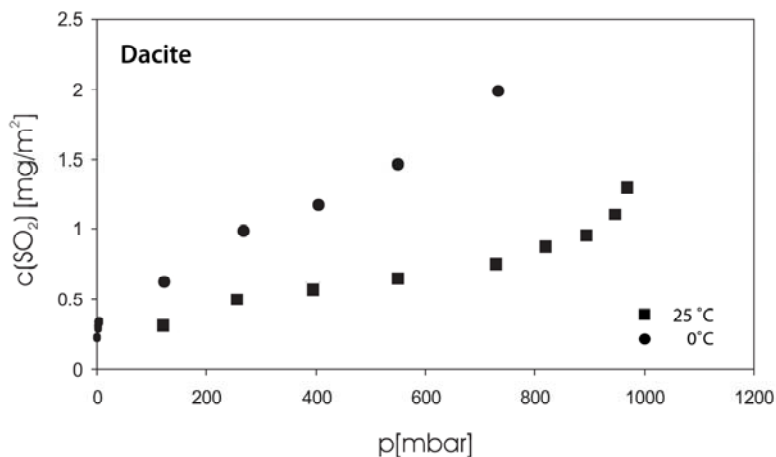


774

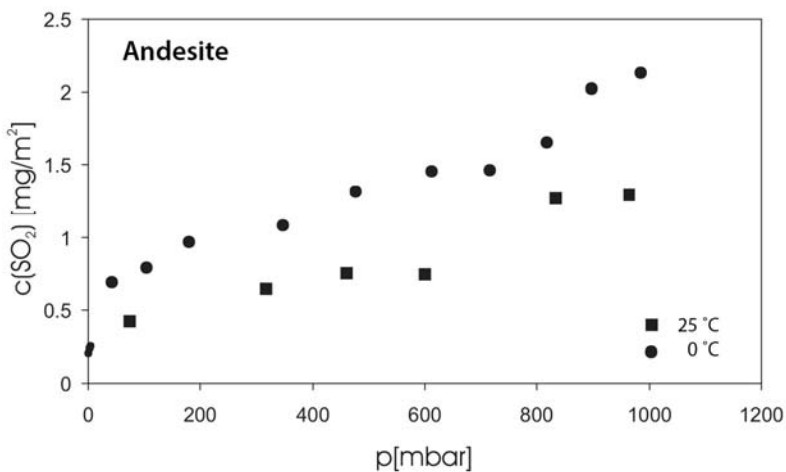
775 **FIGURE 2.** Adsorption and desorption isotherms of SO₂ on glass powders of
776 rhyolitic, dacitic and andesitic composition at 25 °C. Surface concentrations are given
777 in mg per m² surface area. The shape of the adsorption curves corresponds to a “type
778 II” isotherm in the classification of Brunauer (1945); see text for further discussion.
779



780

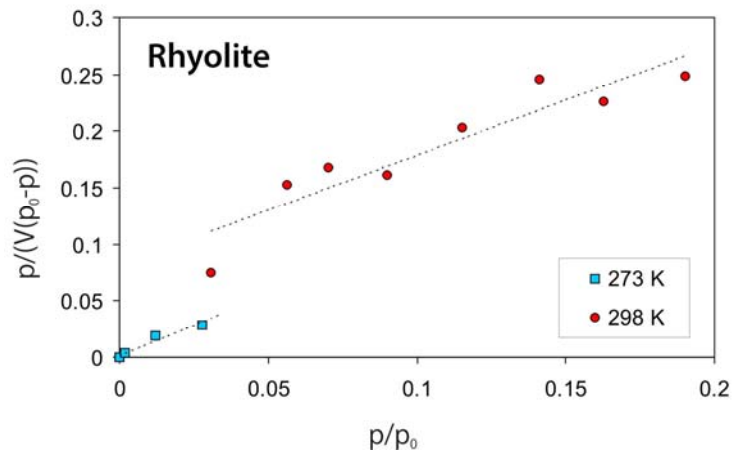


781

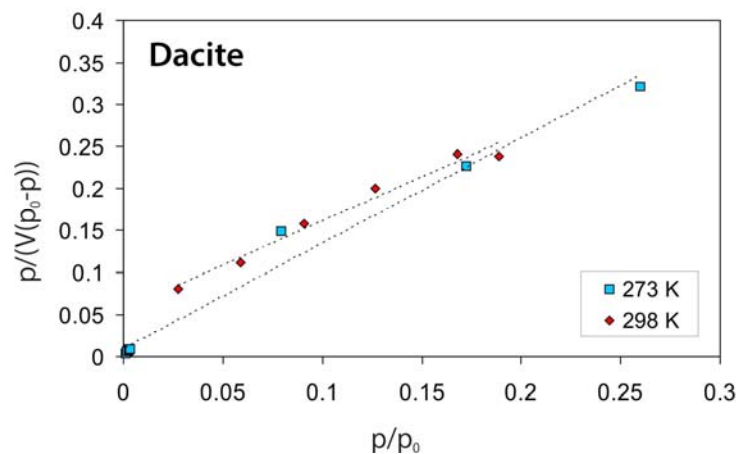


782

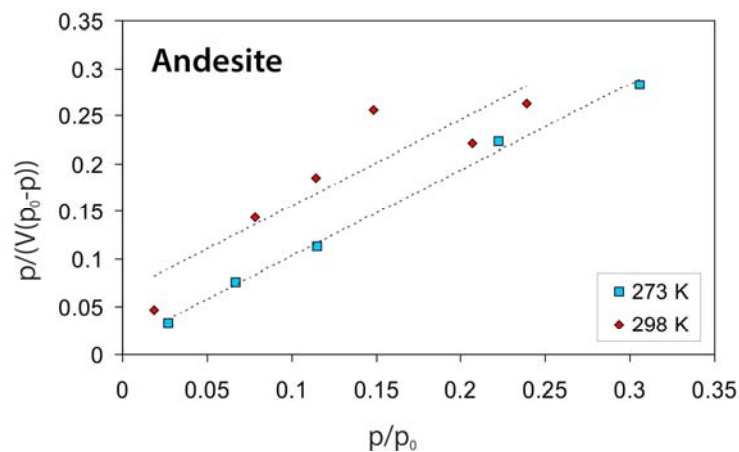
783 **FIGURE 3.** Adsorption isotherms of SO₂ on rhyolite, dacite and andesite glass
784 powder at different temperatures. Adsorption decreases with temperature. Relative
785 errors in measured surface concentration are approximately 20 %.



786

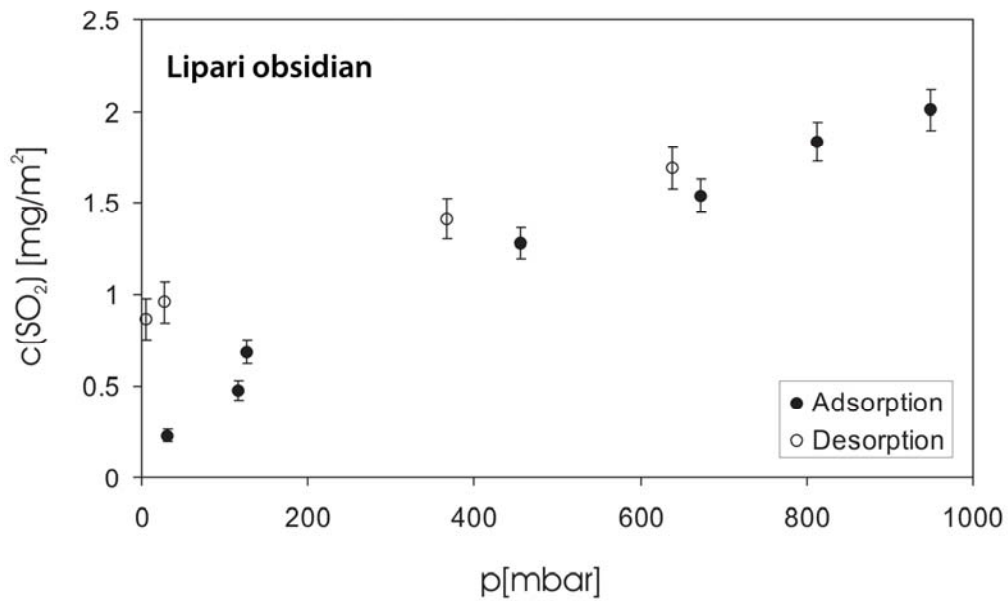


787

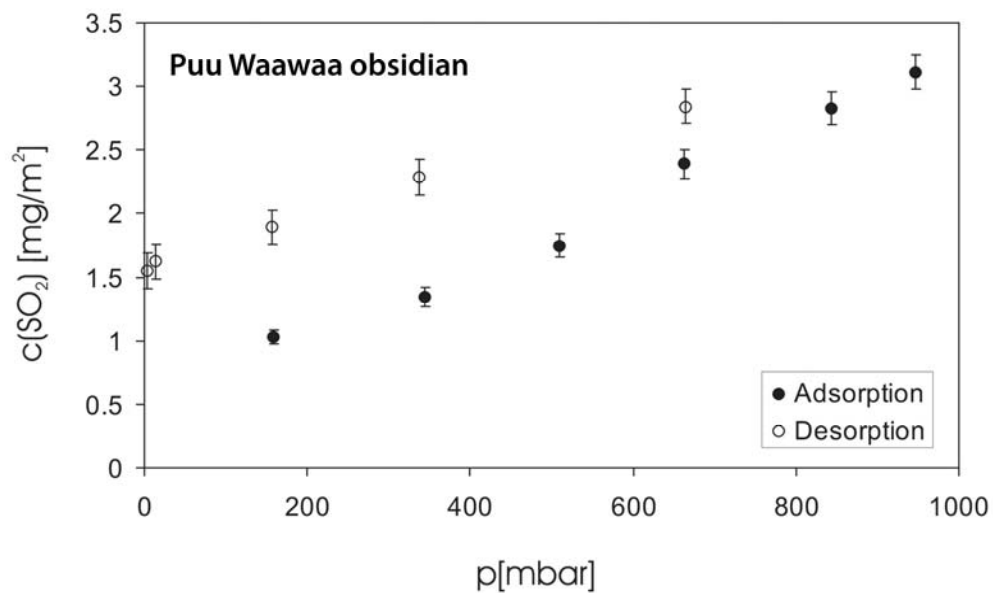


788

789 **FIGURE 4.** BET plots of the adsorption isotherms of SO_2 on rhyolitic, dacitic and
790 andesitic glasses at 0 °C and at 25 °C. V is the volume of adsorbed SO_2 (under
791 standard pressure and temperature) in cm^3/g , p is pressure in mbar and p_0 is the
792 condensation pressure. In this diagram, an adsorption isotherm following the BET
793 equation should plot on a straight line.

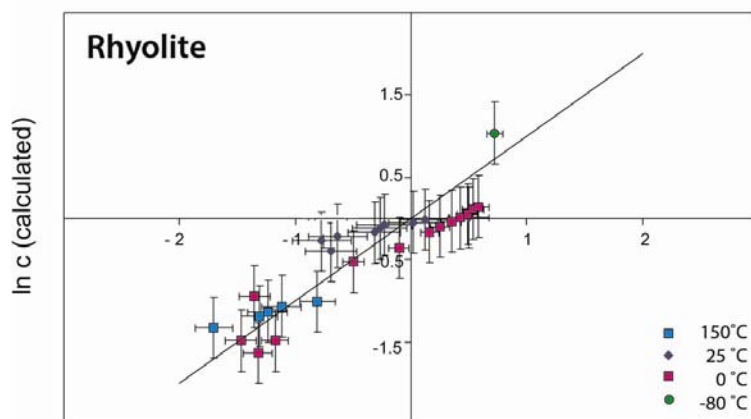


794
795

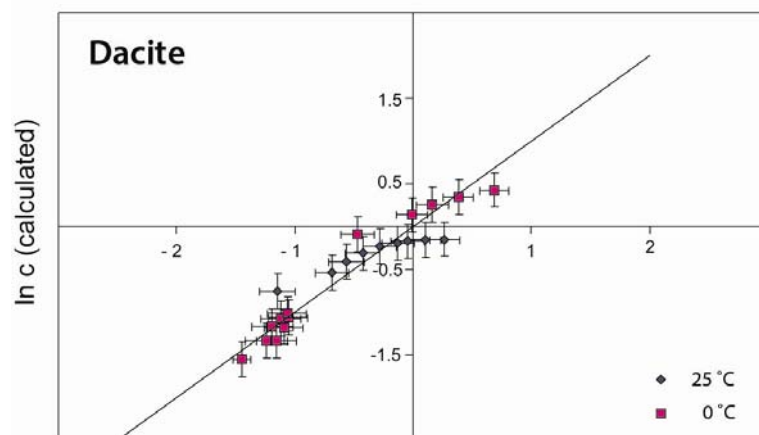


796
797

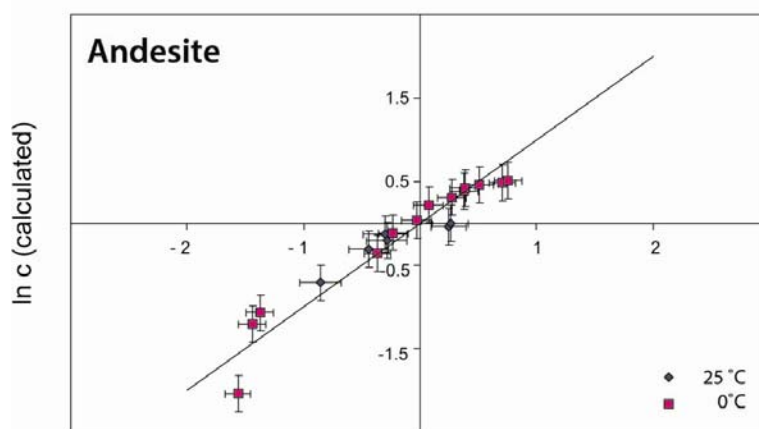
798 **FIGURE 5.** Adsorption and desorption isotherms of SO₂ on powder samples of two
799 natural obsidians, measured at 0°C. The Lipari obsidian (Eolian islands, Italy) is
800 rhyolitic in composition, the Puu Waawaa (Hawaii) obsidian is trachytic.
801



802

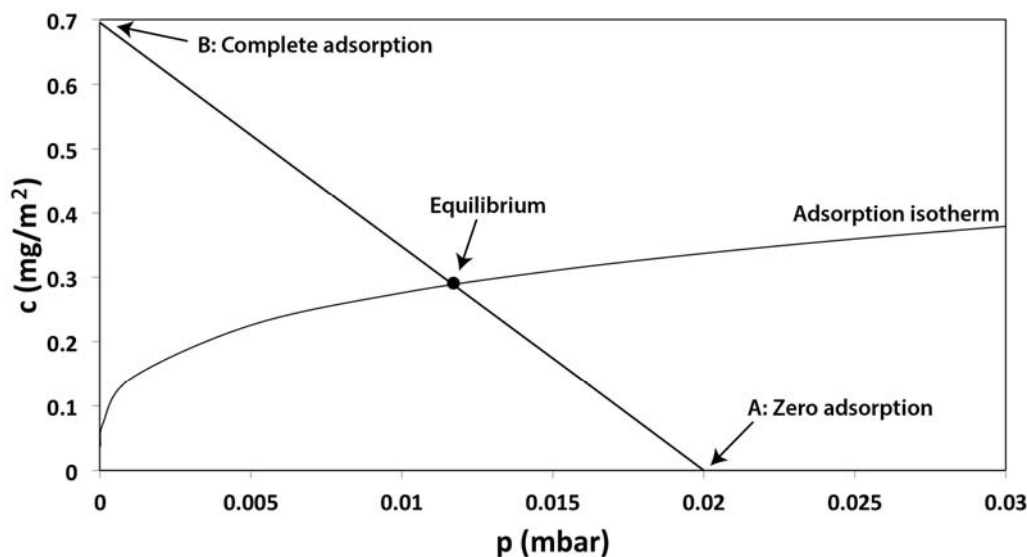


803



804

805 **FIGURE 6.** Comparison of predicted and measured surface concentrations of SO₂ on
806 rhyolitic, dacitic and andesitic glasses. Surface concentrations in mg/m². Error bars
807 for the measurements are the same as in Fig. 2, the errors in the calculated values are
808 derived from the uncertainties in the regression parameters, as given in Table 4.

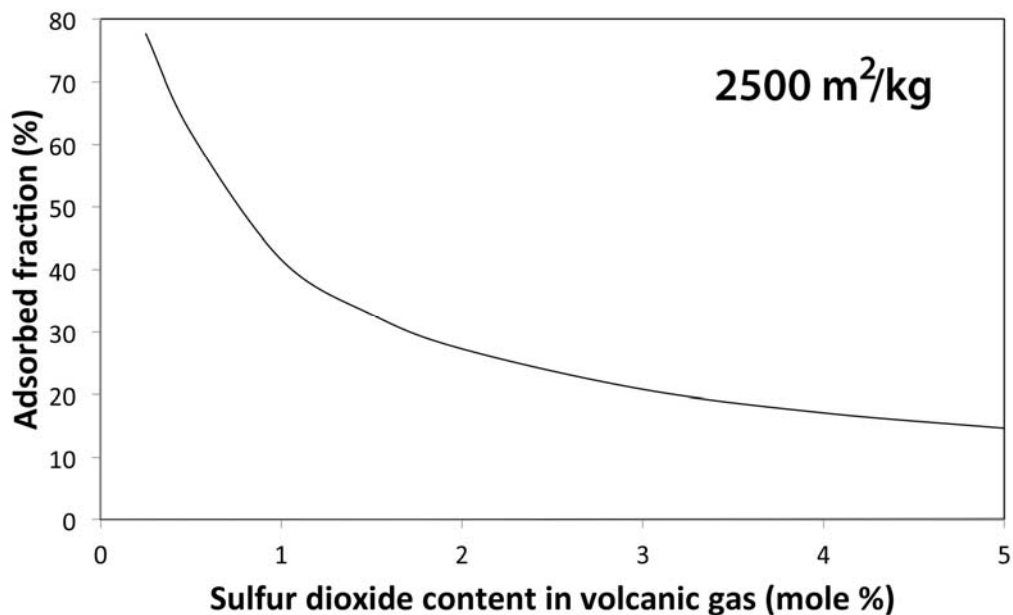


809

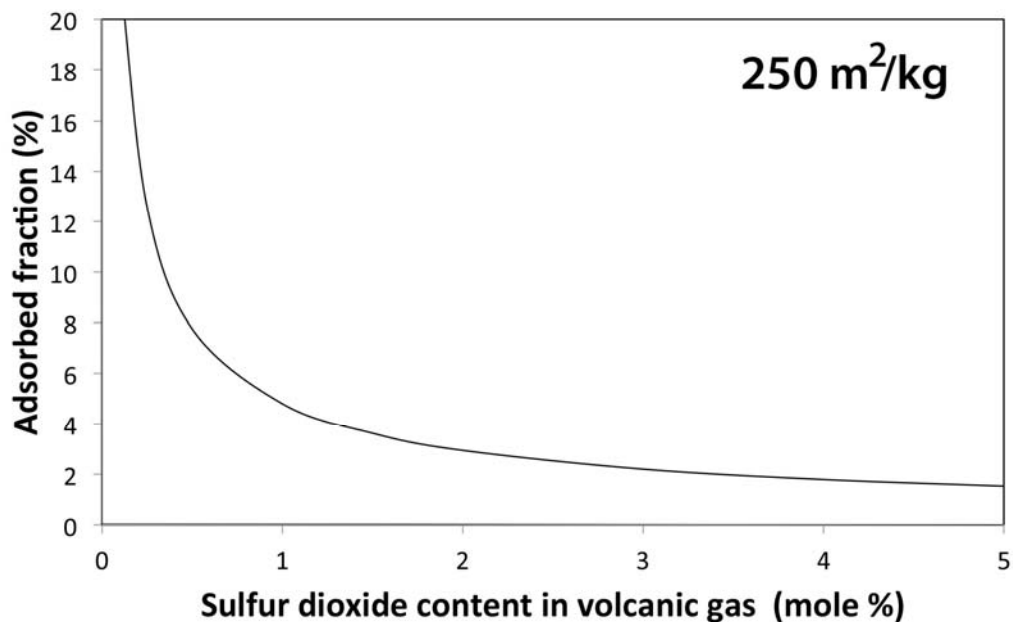
810 **FIGURE 7.** Calculated isotherm for the adsorption of SO_2 on andesite glass at 220 K
811 (-53 °C). The amount of adsorbed SO_2 in equilibrium can be found by the intersection
812 of the isotherm with a straight line connecting the points corresponding to zero
813 adsorption (A) and to complete adsorption (B), respectively. This straight line
814 represents a mass balance for the adsorption process. Assumptions: Specific ash
815 surface of 2500 m^2/kg , weight ratio of volcanic gas (mostly water vapor) to ash of
816 0.05, 1 mole %, SO_2 in the volcanic gas, ratio of air to volcanic gas in the plume 100:
817 1, altitude 10 km. This translates into an initial partial pressure of SO_2 in the diluted
818 plume of 0.02 mbar. For details, see text.

819

820



821
822
823



824
825

826 **FIGURE 8.** Fraction of SO₂ adsorbed on the surface of ash in a volcanic plume as a
827 function of initial SO₂ content, for two different specific surfaces of the ash (2500
828 m²/kg and 250 m²/kg). Assumptions: Weight ratio of volcanic gas to ash of 0.05, ratio
829 of air to volcanic gas in the plume 100: 1, altitude 10 km, temperature 220 K, ash of
830 andesitic composition.

831